November, 1988] © *1988 The Chemical Society of Japan* *Bull. Chem. Soc. Jpn., 61, 3819—3823 (1988)* 3819

Vibrational Analysis of Tangled Spectra. II. Role of Phonon Side Band Structure in the T←S Spectra of Acetophenones

Kenichi NAKASHIMA,† Hiroshi FUTAMI, and Motohiko KOYANAGI*
Department of Chemistry, Faculty of Science, Kyushu University,
Hakozaki, Higashi-ku, Fukuoka 812
(Received May 13, 1988)

$T_{1,2}$←S_0 phosphorescence excitation spectra of acetophenone, acetophenone-*methyl*-d_3, and acetophenone-*phenyl*-d_5 have been observed in the crystals at 4.2 K. Vibration analysis for the observed tangled spectra becomes possible only by the help of calculations which allow untangling of the tangled spectra. The calculations involve interstate mixings, by vibronic and environmental interactions, among 36 crude adiabatic Born-Oppenheimer vibronic functions of $^3\pi\pi^*$ and $^3n\pi^*$ states. A new aspect of the present work is introduction of a role of intermolecular phonon side bands into the calculations; this clearly showing that the observed spectra are reproduced much better than unless otherwise.

In the preceding paper,1) we analyzed the tangled $T_{1,2}$←S_0 spectrum of acetophenone in the crystal and showed how conventional analysis was of no use for such a tangled system. Qualitatively, the band structure was explained in terms of canonical mixture of 36 BO vibronic functions of the T_1 and T_2 states. However, several disparities remained unsettled between the observed and the calculated spectrum. These are: (i) an abrupt decrease in calculated intensity in the zeroth order 0–0 band region of the $T_2(n\pi^*)$←S_0 transition, (ii) a discrepancy in the overall spectral intensity distributions, (iii) the lack of several structured bands in the calculation, etc.

In the present paper we report on three items. The first is to give the experimental $T_{1,2}$←S_0 absorption spectra of acetophenone-*methyl*-d_3 (hereafter abbreviated as $\mathbf{d_3}$) and acetophenone-*phenyl*-d_5 ($\mathbf{d_5}$). To our knowledge, no experimental data thereof have been reported. The second is to simulate these spectra by means of a similar method as given previously for $\mathbf{d_0}$.1) The third is to take fully into account intermolecular phonon side bands. The simulation with such a phonon correction leads to a great improvement over the earlier one. At least, the extent of the disparities (i) and (ii), loc. cit., seems to be greatly diminished.

Experimental

The guest molecules, nonlabeled acetophenone ($\mathbf{d_0}$, a GR grade reagent from Tokyo Kasei Co.) and $\mathbf{d_3}$ and $\mathbf{d_5}$ (both reagents from Merck, Sharp and Dohme of Canada), were purified by distillation in vacuo. All T←S phosphorescence excitation and absorption spectra were observed at 4.2 K in the crystals. For the measurements of the excitation spectra, ca. 10^{-3} M§ benzaldehyde was doped as an effective phosphorescence emitter while for the absorption measurements, pure crystals with ca. 5 mm thickness were used. All spectra were recorded on a 3/4 m Nalumi Spectrometer with an HTV R375 photomultiplier tube. Other experimental details were similar to those described elsewhere.1,2)

Theoretical

First, $T_{1,2}$←S_0 spectra of the two deuterated acetophenones were simulated in almost all the same way as reported for $\mathbf{d_0}$.1) Some suitable frequency changes for many fundamental vibrations were made according to the same procedure as given for benzaldehydes.2) The exceptions are in the determination of three out-of-plane vibrational frequencies of T_1: ν'_{43}, ν'_{42}, and ν'_{41}. The modes, especially ν''_{43} and ν''_{41}, have been well known to be delocalized over the ring and C–$COCH_3$ framework.1,3–6) Furthermore, it is expected that a large increase in the C–(CXO) bond order consequent to π^*←π promotion leads to an increase in the CXO-wagging vibrational frequency on going from the ground to the $\pi\pi^*$ excited state. For these reasons, the three diagonal matrix elements were treated as independent parameters. Crystal field and vibronic interaction matrix elements were determined on the basis of the phosphorescence intensity data for mixed isotopic crystal systems.2) The final data employed for $\mathbf{d_3}$ are partially given in Tables 1 and 2. For $\mathbf{d_5}$, a part of only the diagonal elements are given in Table 1.

Secondly, intermolecular phonon bands were taken into account for the explanation of a broad, but some structured, background absorption which is presumed to dominate a large part of the total absorption intensity. It is found that a similar sub-structure always attends both on almost all prominent phosphorescence bands and on several absorption bands. On the assumption that this was due to a pile of Franck–Condon (FC) type phonon bands, we synthesized a model function for such a feature on a computer by using ten independent gaussians. The three parameters of each gaussian (i.e., location of the frequency center, weight, and bandwidth) were chosen so that the origin band structure of each T←S spectrum was reproduced as best as possible. A final model structure for $\mathbf{d_0}$ is shown in Fig. 1.

The first few bands in the T←S spectra of $\mathbf{d_3}$ and $\mathbf{d_5}$ were sharper than those in $\mathbf{d_0}$ (as demonstrated in Fig.

---

† Present address: Laboratory of Chemistry, College of Liberal Arts, University of Saga, Honjo, Saga 840.

§ 1 M=1 mol·dm^{-3}.

Table 1. Zeroth Order Diagonal Matrix Elements Employed for Acetophenone, Acetophenone-*methyl*-d_3, and Acetophenone-*phenyl*-d_5[a)]

Band	$\Delta\tilde{\nu}/\mathrm{cm}^{-1}$[b)]			Band	$\Delta\tilde{\nu}/\mathrm{cm}^{-1}$[b)]			Band	$\Delta\tilde{\nu}/\mathrm{cm}^{-1}$[b)]		
	$\mathbf{d_0}$	$\mathbf{d_3}$	$\mathbf{d_5}$		$\mathbf{d_0}$	$\mathbf{d_3}$	$\mathbf{d_5}$		$\mathbf{d_0}$	$\mathbf{d_3}$	$\mathbf{d_5}$
$\lvert 0\rangle$	0	0	0	$\lvert 27\rangle$	590	535	570	$\lvert 45^*\rangle$	*50*	*45*	*50*
$\lvert 45\rangle$	70	70	65	$\lvert 40\rangle$	600	590	465	$\lvert 44^*\rangle$	*125*	*110*	*125*
$\lvert 44\rangle$	90	85	90	$\lvert 39\rangle$	700	685	565	$\lvert 30^*\rangle$	*170*	*160*	*170*
$\lvert 30\rangle$	190	185	185	$\lvert 38\rangle$	735	715	620	$\lvert 43^*\rangle$	*195*	*180*	*195*
$\lvert 43\rangle$	245	270	225	$\lvert 37\rangle$	835	800	675	$\lvert 29^*\rangle$	*360*	*305*	*360*
$\lvert 41\rangle$	325	340	290	$\lvert 36\rangle$	930	880	800	$\lvert 42^*\rangle$	*380*	*360*	*340*
$\lvert 29\rangle$	360	355	370	$\lvert 35\rangle$	970	965	980	$\lvert 41^*\rangle$	*430*	*390*	*375*
$\lvert 42\rangle$	445	445	425	$\lvert 0^*\rangle$	*0*	*0*	*0*	$\lvert 27^*\rangle$	*550*	*495*	*550*

a) Only the representative vibronic levels are shown here. Asterisked states denote the BO vibronic levels of $T_2^0(n\pi^*)$ and the others $T_1^0(\pi\pi^*)$. b) Diagonal matrix elements are calculable on the basis: for $\mathbf{d_0}$, $\lvert 0\rangle \leftrightarrow 26150$ cm^{-1} and $\lvert 0^*\rangle \leftrightarrow 26555$ cm^{-1}; for $\mathbf{d_3}$, $\lvert 0\rangle \leftrightarrow 26145$ cm^{-1} and $\lvert 0^*\rangle \leftrightarrow 26560$ cm^{-1}; and for $\mathbf{d_5}$, $\lvert 0\rangle \leftrightarrow 26225$ cm^{-1} and $\lvert 0^*\rangle \leftrightarrow 26575$ cm^{-1}. Underlined values give energy separation from the $\lvert 0^*\rangle$ level.

Table 2. Off-Diagonal Matrix Elements Employed for Acetophenone-*methyl*-d_3[a)]

T_1	T_2								
	$\lvert 0^*\rangle$	$\lvert 30^*\rangle$	$\lvert 29^*\rangle$	$\lvert 27^*\rangle$	$\lvert 45^*\rangle$	$\lvert 44^*\rangle$	$\lvert 43^*\rangle$	$\lvert 42^*\rangle$	$\lvert 41^*\rangle$
$\lvert 0\rangle$	70.00	17.15	7.00	33.60	25.67	43.18	23.38	85.00	36.21
$\lvert 30\rangle$	17.15	4.20	1.71	8.23	6.29	10.58	5.73	20.82	8.87
$\lvert 27\rangle$	33.60	8.23	3.36	16.13	12.32	20.73	11.22	40.80	17.38
$\lvert 45\rangle$	25.67	6.29	2.57	12.32	0	0	0	0	0
$\lvert 44\rangle$	43.18	10.58	4.32	20.73	0	0	0	0	0
$\lvert 43\rangle$	26.08	6.39	2.61	12.52	0	0	0	0	0
$\lvert 42\rangle$	85.00	20.82	8.50	40.80	0	0	0	0	0
$\lvert 41\rangle$	36.21	8.87	3.62	17.38	0	0	0	0	0
$\lvert 40\rangle$	8.50	2.08	0.85	4.08	0	0	0	0	0
$\lvert 39\rangle$	8.50	2.08	0.85	4.08	0	0	0	0	0
$\lvert 38\rangle$	36.21	8.87	3.62	17.38	0	0	0	0	0
$\lvert 45+30\rangle$	6.29	1.54	0.63	3.02	0	0	0	0	0
$\lvert 44+30\rangle$	10.54	2.58	1.05	5.06	0	0	0	0	0
$\lvert 43+30\rangle$	5.69	1.40	0.57	2.73	0	0	0	0	0
$\lvert 42+30\rangle$	20.82	5.10	2.08	10.00	0	0	0	0	0

a) Only the representative elements are given here although 99X99 values are employed for the calculations. In cm^{-1} units.

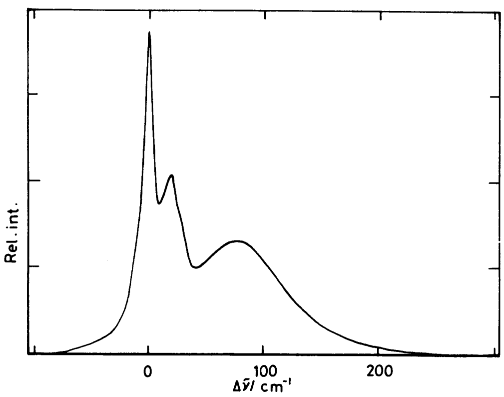

Fig. 1. A model shape function for the background FC type phonons. The fundamental zero-phonon line at $\Delta\nu=0$ cm^{-1} is lorentzian with $\Gamma_{\mathrm{fwhm}}=10$ cm^{-1} while the other part is synthesized using ten different gaussian functions with various values of Γ_{fwhm}.

2). We thus assumed that each fundamental band of the former had a lorentzian shape with a 7 cm^{-1} fwhm while that of the latter a 10 cm^{-1} fwhm.

Results and Discussion

T←S Phosphorescence Excitation Spectra of the Deuterated Acetophenones. The observed T←S phosphorescence excitation spectra of $\mathbf{d_3}$ and $\mathbf{d_5}$ in the crystals[7)] are shown in Fig. 2. For comparison, the spectrum of $\mathbf{d_0}$ is added. At glance, most intensive bands of each spectrum appear to display one-to-one correspondence. However, the correspondence is in appearance only (vide infra).

The prominent band at the longest wavelength (26112 cm^{-1} for $\mathbf{d_3}$ and 26177 cm^{-1} for $\mathbf{d_5}$) is assigned to the T_1 origin band of the $T_1(\pi\pi^*)\leftarrow S_0$ transition. Energy closeness between the phosphorescence origin band of $\mathbf{d_3}$ in $\mathbf{d_5}$ (at 26099 cm^{-1})[3)] and the crystal absorption origin band (at 26112 cm^{-1}) seems to support this assignment. The large (ca. 70 cm^{-1})

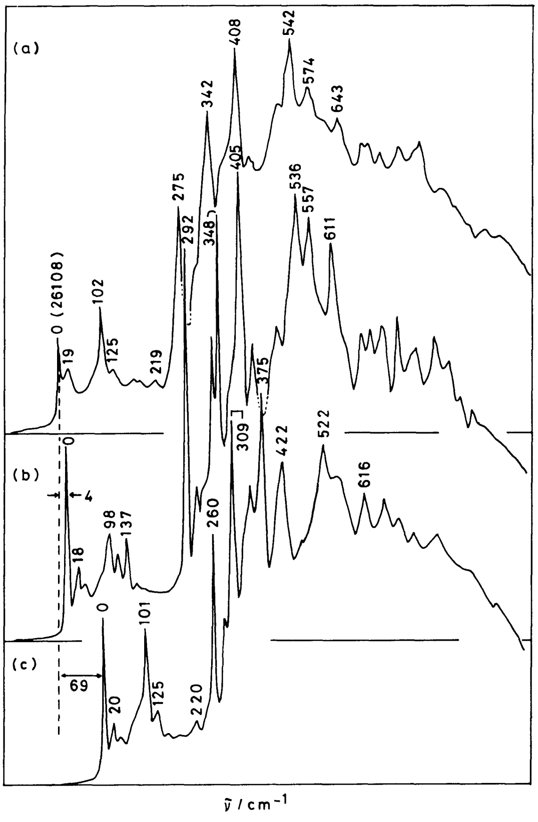

Fig. 2. Observed T←S phosphorescence excitation spectra of (a) (**d**$_0$), (b) **d**$_3$, and (c) **d**$_5$ in the crystals at 4.2 K.

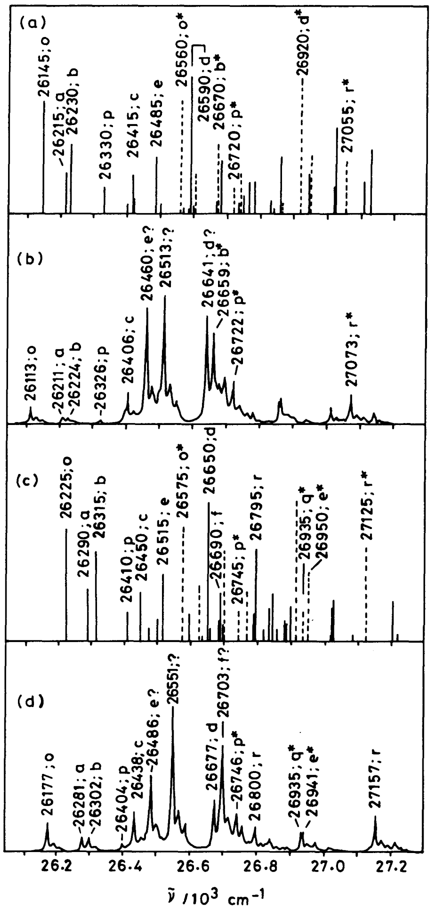

Fig. 3. (a, c) Zeroth order levels employed and (b, d) simulated T←S spectra at 0 K. (a, b) For **d**$_3$; and (c, d) for **d**$_5$. For band designations, see Ref. 1.

origin band deuteration shift on going from **d**$_0$ to **d**$_5$ allows assignment of the lowest excited triplet state to $\pi\pi^*$ since a similar deuteration shift has been established for the $\pi\pi^*$ transition of benzaldehyde-*phenyl*-d_5.[8] The very small (4 cm^{-1}) deuteration shift in **d**$_3$ gives another piece of evidence for the validity of the $\pi\pi^*$ assignment.

Satellite bands were observed for all T←S spectra at ca. 20, ca. 40, and ca. 90 cm^{-1} from each origin band (and also first several strong false origins) to the higher wavenumber side. Similar sub-structured bands to the lower wavenumber side have also been observed in T→S spectra.[3] These are assigned to lattice vibrations in a similar way to the cases of T←S and T→S electronic spectra of *p*-dihalobenzenes[9] and *p*-benzoquinone[10] in the pure and isotopic mixed crystals. No evidence is obtained for alternative assignments: e.g., either trap bands or Davydov splitting components. The observed band broadness never contradicts our interpretation.

The bands in the 90—140 cm^{-1} region are quite interesting, but complicated (especially for **d**$_3$). Such small frequencies may generally be ascribed to two torsional vibration modes, i.e., τ (-COCH$_3$) and τ (-CH$_3$). Although no information has been presented about these potential surfaces of the crystal phase acetophenones both for the ground and for the excited state, the reasonably sharp origin bands observed both in the phosphorescence and in the excitation spectrum suggest that the rotational potential barriers thereof are high relative to those for the S$_1$(nπ^*) state: The S$_1$(nπ^*)←S$_0$ phosphorescence excitation spectra in the pure crystal and mixed crystals showed all poorly resolved features.[11,12] Recent jet works[13—15] may be helpful for obtaining information on those potentials.[16]

Simulated T←S Spectra of d$_3$ and d$_5$ in the Crystal. The zeroth order levels of **d**$_3$ and **d**$_5$ are shown in Figs. 3a and 3c, respectively. The height of the solid lines represents the relative value of the interaction between two levels of T$_1$(0,0+ν_i) and T$_2$(0–0); and that of the dashed lines the interaction between the levels of T$_1$(0–0) and T$_2$(0,0+ν_i). Refined calculation spectra of the two deuterated compounds are shown in Figs. 3b and 3d, respectively (for the observed spectra, see Figs. 2b and 2c). The eigenfunction corresponding to each calculated origin band (at 26113 cm^{-1} for **d**$_3$ and 26177 cm^{-1} for **d**$_5$) is approximately described by

$$|26113\rangle = 0.18|0^*\rangle - 0.96|0\rangle + 0.10|42^*\rangle + \cdots \quad (1)$$

and

$$|26177\rangle = 0.23|0^*\rangle - 0.93|0\rangle + 0.12|42^*\rangle + \cdots. \qquad (2)$$

A significant mixing of $|0^*\rangle$ with $|0\rangle$ is clear for each case. This explains why the origin band appears with remarkable intensity despite its substantial $\pi\pi^*$ character.

In contrast to the above, there is no convincing band which is assignable to the origin band of the $T_2(n\pi^*)\leftarrow S_0$ transition. Here we give only three eigenfunctions. These may be combined with three of the most intensive observed bands (see also Figs. 2b, 2c, 3b, and 3d):

for $\mathbf{d}_3$,

$$|26460\rangle = 0.75|41\rangle + 0.32|42\rangle - 0.45|0^*\rangle + \cdots \qquad (3)$$

$$|26513\rangle = 0.61|41\rangle - 0.55|42\rangle + 0.47|0^*\rangle + \cdots \qquad (4)$$

$$|26641\rangle = 0.62|42\rangle - 0.52|27\rangle + 0.44|0^*\rangle + \cdots, \qquad (5)$$

and for $\mathbf{d}_5$,

$$|26486\rangle = 0.62|41\rangle + 0.45|44 + 30\rangle - 0.36|0^*\rangle + \cdots \qquad (6)$$

$$|26551\rangle = 0.59|41\rangle - 0.46|42\rangle + 0.51|0^*\rangle + \cdots \qquad (7)$$

$$|26703\rangle = 0.46|40\rangle + 0.57|41 + 31\rangle + 0.39|0^*\rangle + \cdots, \qquad (8)$$

Despite superficial one-to-one band correspondence between the observed prominent bands of $\mathbf{d}_3$ and those of $\mathbf{d}_5$, there are considerable differences between the relevant calculated eigenvector-components of the two compounds as well as between the expansion coefficients of the corresponding components (e.g., compare Eq. 3 with Eq. 6 and Eq. 5 with Eq. 8). A similarity of these results for acetophenones to other results for aromatic aldehydes[2,17,18] leads us to a deduction that this kind of mixing is general for a molecule with a lower excited state of a strongly forbidden character. This deduction is important.

Role of Background Phonon Bands. If discussion is restricted to the spectral intensity distribution, the mimicking is poor. Here let us put aside an obvious experimental fact that spectral bands become broader on going toward shorter wavelengths. To be noted is a big difference between the observed and the calculated spectral intensity distributions: e.g., an abrupt decrease in intensity of the calculated spectra in the zeroth order 0–0 band region of the $T_2(n\pi^*)\leftarrow S_0$ transition and another decrease in intensity of 26.7—$26.8\times10^3\,\mathrm{cm}^{-1}$ region bands. In order to find a solution to the disparity, we introduced an intermolecular phonon ensemble to the calculations. The ensemble is presumed to closely concern a pile of FC type phonon vibrations.

The model structure employed is shown in Fig. 1. The revised calculation is then straightforward. The resultant spectrum for $\mathbf{d}_0$ is shown in Fig. 4 together with the uncorrected spectrum. Clearly, the revised spectrum is much close to the observed one. However, a question might be raised: Is such a band feature as shown in Fig. 1 due to another FC structure? Instead of the assumed intermolecular lattice vibrations, there are two intramolecular vibrations with small frequency as what comes under this category: the ϕ-$COCH_3$ tortional (i.e., ν_{45}) and the CH_3-rotational vibration (ν_{44}). As regards this, we have no unambiguous evidence which discriminates between them. However, we know that similar broad features also do appear for several other aromatic aldehydes with high τ (ϕ-CHO) potential barriers[2,4,17] and, further, almost all of these are explainable by FC-type phonon bands.[18] We are thus inclined to conclude that the substructure in the acetophenone crystal is also mostly explained by FC type intermolecular phonons.

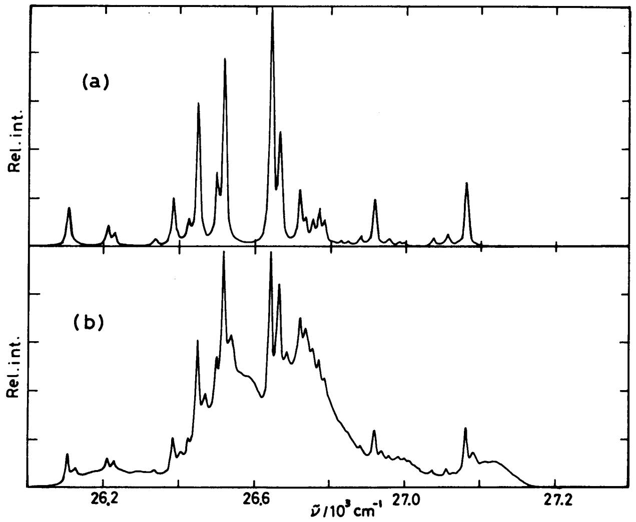

Fig. 4. Simulated T←S spectra of $\mathbf{d}_0$ at 0 K. (a) Without and (b) with the background phonon structure introduced (see the text and Fig. 1). Figure 4a is the same one as reported previously (cf. Fig. 4b of Ref. 1).

The calculations reported in this paper were carried out at the Computation Center of Kyushu University. This work was in part supported by a Grant-in-Aid from the Ministry of Education, Science and Culture (No. 62540358).

References

1) K. Nakashima and M. Koyanagi, *Bull. Chem. Soc. Jpn.*, **58**, 2000 (1985). Paper I of this series.

2) M. Koyanagi, K. Nakashima, and L. Goodman, *Chem. Phys.*, **92**, 435 (1985).

3) M. Koyanagi, R. J. Zwarich, and L. Goodman, *J. Chem. Phys.*, **56**, 3044 (1972).

4) L. Goodman and M. Koyanagi, *Mol. Photochem.*, **4**, 369 (1972).

5) A. Gambi, S. Giorgianni, A. Passerini, R. Visinoni, and S. Ghersetti, *Spectrochim. Acta,* **36A**, 871 (1980).

6) A. J. Duben, L. Goodman, and M. Koyanagi, "Excited States," ed. by E. C. Lim, Academic Press, New York and London (1974), Vol. 1, p. 295.

7) Each phosphorescence excitation spectrum at 4.2 K was confirmed to be very close to the corresponding direct T←S absorption spectrum at the same temperature.

8) M. Koyanagi and L. Goodman, *Chem. Phys.,* **39**, 237 (1979).

9) G. Castro and R. M. Hochstrasser, *J. Chem. Phys.,* **46**, 3617 (1967).

10) M. Koyanagi, Y. Kogo, and Y. Kanda, *J. Mol. Spectrosc.,* **34**, 450 (1970).

11) W. A. Case and D. R. Kearns, *J. Chem. Phys.,* **52**, 2175 (1970).

12) Despite many trials, only considerably broad bands were observed for the $S_1(n\pi^*)\leftarrow S_0$ spectra of acetophenone in the crystal and in mixed crystals at 1.8 and 4.2 K. This is in big contrast to the T→S phosphorescence and T←S excitation spectra of acetophenone itself [and the $S_1(n\pi^*)\leftarrow S_0$ spectra of benzaldehyde (see Ref. 4)]. The hosts employed were deuterated acetophenones, methylbenzoate, benzoic acid, pentane, hexane, methylcyclohexane, and benzene. See also Ref. 16 for a similar problem.

13) N. Omori, T. Suzuki, and M. Ito, *J. Phys. Chem.,* **92**, 1086 (1988).

14) J. L. Tomer, J. H. Spangler, and D. W. Pratt, *J. Am. Chem. Soc.,* **110**, 1615 (1988).

15) E. Villa, A. Amirav, W. Chen, and E. C. Lim, *Chem. Phys. Lett.,* **147**, 43 (1988).

16) Aside from several minor points, recently reported supersonic jet $T_1\leftarrow S_0$ spectra of acetophenone (Refs. 13 and 14) are in good accord with the predicted spectra (Ref. 19), one of which (the case of $\Delta E\approx -405\,\mathrm{cm}^{-1}$ in the crystal where the minus means $T_1={}^3n\pi^*$) was demonstrated previously (see Fig. 5 in Ref. 1). Our preliminary calculation for the same system, but with $F_e=0$ (gas model), also shows that an almost similar band pattern is realized when $\Delta E[({}^3n\pi^*)-({}^3\pi\pi^*)]$ is small (say, less than $200\,\mathrm{cm}^{-1}$). However, a problem is that there never appear remarkably intense two bands in the 70—90 cm^{-1} region in contrast to the observed jet spectra. According to our rough estimation, smallness in ν''_{45} frequency (e.g., $44\,\mathrm{cm}^{-1}$ according to Ref. 3) requires that any jet experiments for a molecule with such a small fundamental frequency must be done at very low vibrational temperature [say, less than 20 K, at least, to attain a relation of I(hot-band system)<0.1×I(cold-band system)]. Because we believe that the S←S and a large part of the T←S jet spectrum of benzaldehyde (Ref. 13 and private communications from Prof. D. W. Pratt) quite resemble the corresponding spectra in methylcyclohexane matrices at 4.2 K (see Refs. 4, 6, 17 for the assignments and discussion), we wonder if an analogous discussion might be possible also for the acetophenone cases. For making the points clear, an investigation on the simulation T←S spectra of the vapor phase acetophenone is in progress.

17) M. Koyanagi, H. Futami, and K. Nakashima, *J. Chem. Phys.,* **89**, 2662 (1988).

18) H. Futami, Master Thesis, Kyushu University, 1988; H. Futami and M. Koyanagi, *Mem. Fac. Sci. Kyushu Univ., Ser. C,* **16**, 101 (1988).

19) K. Nakashima, Doctoral Disertation, Kyushu University, 1985, Chap. 5.